Excluded-volume descriptors for dipole-bound anions: Amine N-oxides as a test case

Thomas Sommerfeld[1, a)] and Megan C. Davis[1]

Department of Chemistry and Physics, Southeastern Louisiana University, SLU 10878, Hammond, LA 70402, USA

(Dated: 11 January 2020)

Dipole-bound anions can be theoretically characterized at three fundamentally different levels. The highest are *ab initio* calculations, which themselves range from fairly approximate, say, Koopmans's Theorem (KT) or MP2, to highly sophisticated, say, electron affinity EOM-CCSDT, which rivals experiments in reliability. The next level down is represented by one-electron model Hamiltonians. Again, one-electron model Hamiltonians can be fairly approximate, especially if the molecular system is modeled by a simple point-dipole and point-polarizable site; however, very reliable models have been developed for specific systems, for example, water clusters. At the lowest level, one can qualitatively explain trends in classes of dipole-bound anions in terms of the dipole moment, μ, the polarizability, α, and the so-called excluded volume, V_x.

This project aims at the qualitative level. While the dipole moment and the polarizability possess clear-cut definitions, the excluded volume must—similar to all molecular volumes—remain a rather vaguely defined term, and so far we are unaware of any quantitative definition in the literature. Here we introduce and investigate three descriptors for V_x. To this end, we first establish a data set with consistent *ab initio* results for 25 amine N-oxides structures. Then we demonstrate that the descriptors are indeed able to explain trends for sets of isomers and conformers and investigate to what extent the descriptors are able to predict electron binding energy of dipole-bound states using simple quantitative structure-property relationship-like models. It turns out that μ and V_x provide a reasonably accurate prediction of the electrostatic part of the electron bind energy (the KT value) and that the polarizability α provides an acceptable prediction of the electron correlation contribution.

[a)]Electronic mail: Thomas.Sommerfeld@selu.edu

I. INTRODUCTION

It is useful to divide anions into two major classes: valence and non-valence anions. In a valence anion, the excess electron occupies a compact valence orbital showing a spatial extent comparable to the nuclear framework. In contrast, in a non-valence anion, the excess electron occupies a spatially extended orbital largely localized outside the valence region, that is, outside the van der Waals surface of the neutral molecule.

Examples for valence anions are stable closed-shell anions such as OH^- or NO_3^- known from solution and atmospheric chemistry or radical anions such as the quinone anion[1,2]. Examples for non-valence anions are dipole-bound anions (an excess electron attached to the molecular dipole)[3,4], correlation-bound anions (an excess electron unbound in Hartree-Fock but bound in correlated calculations)[5,6], doubly-Rydberg anions (two excess electrons bound to a positive core)[7,8], as well as solvated-electron states in the widest sense (see e.g. the recent review[9]). We emphasize that these two classes correspond to extremes on a continuous scale, because, on the one hand, valence and non-valence states can mix and, on the other hand, a valence state can evolve into a non-valence state, and in these more general cases it is more appropriate to speak of the valence or non-valence "character" of an anionic species.

Dipole-bound anions have been extensively studied for many decades[1,3,4,9] and probably represent the best-characterized subclass of non-valence states. The name "dipole-bound" itself originates from the leading electrostatic term in an "intermolecular interaction-style" analysis, yet, instead of two molecules, the interaction between a neutral and an electron is analyzed.

A detailed quantitative analysis in this spirit can be based on the comparison of computed binding energies with different *ab initio* methods[10,11]. In this scheme, the most useful comparison is probably that of the Koopmans's Theorem (KT) value for the electron binding energy E_b with a reliable value from a coupled-cluster with single, double, and perturbative triple substitutions (CCSD(T)), or equation-of-motion couple-cluster with single and double substitutions (EOM-CCSD) calculation: KT treats exchange-repulsion and electrostatic interactions between a neutral described by Hartree-Fock theory and an excess electron. It defines therefore an electrostatic picture of a dipole-bound anion.

If electron correlation is then "switched on" at the CCSD(T) or EOM-CCSD level or

higher, typically a reliable fixed-nuclei value of E_b is obtained. These reliable binding energies tend to be substantially higher than the associated KT values, however, the percent-change is strongly molecule dependent. In fact, correlation-bound states are a limiting case of this trend showing a 100% increase. In any event, based on two *ab initio* electron binding energies—the approximate KT and one reliable value—the total electron binding energy can be split into an electrostatic and a correlation contribution.

An alternative theoretical description of dipole-bound states is provided by one-electron model potentials and the associated one-electron model Hamiltonians. Generic one-electron models typically consist of a point-dipole, a point-polarizable site, and a repulsive potential (see, e.g.,[12–14]), yet finite dipoles and polarizability models based on Drude oscillators (charge-on-a spring models) represent other choices. More sophisticated one-electron models have been developed for specific systems, including water[15,16], methanol[17], and ammonia clusters[18], and these models can be highly competitive especially for large systems. Since it is possible to study the impact of switching on or off any part of the electron-molecule interaction, one-electron model potentials may also be used for interpretative purposes. Regarding the current context, however, we make use of an approximate closed-form solution of a particular simple model[14]; we will come to this point in section III.

Last, much insight has been gained from a qualitative conceptual framework developed by comparing different molecules in related families. In retroperspective, it is hardly surprising that apart from the dipole moment, electron binding energies of non-valence states are impacted by the molecular polarizability and the excluded volume[3,19]. Loosely speaking, the dipole moment may be the leading electrostatic term in a long-range expansion, however, first, the binding energy is equally determined by intermediate and short-range interactions, and second, the dipole moment may be small, while other terms may be large.

At intermediate distances, the molecular polarizability may contribute substantially to the attractive interaction, and the short-range repulsion is characterized by the excluded volume: Consider, for example, a molecule, where the molecular dipole is associated with a certain functional group, say a cyano or nitro group. Depending on the molecular structure, the excess electron may then be able to easily access the positive end of this substructure, or it may be crowded out by other fairly non-polar groups. The volume where Pauli-repulsion associated with this crowding effect is noticeable, is referred to as excluded volume.

Examples clearly demonstrating the excluded volume effect are $(H_2O)_2Ar_N^-$ clusters,

where Ar atoms crowd the positive end of the $(H_2O)_2$ dipole[19], electrons dipole-bound to nitriles, where increasing subsitution at the α carbon leads to higher dipoles but lower binding energies[3], and the 2s-like electron in $Li(NH_3)_N$ $(N = 0 - 4)$ clusters, which is increasingly pushed outside of the first solvation shell of a Li^+ cation[20]. On the other hand, a recent study of electron detachment from para-substituted alkyl-phenolate ions (the dipole-bound state is an excited state of the anion and gets populated during the photodetachment experiment) shows effectively no influence of the alkyl chain length on the spectroscopic signature of the dipole-bound state[21]. While we have no definite explanation for this observation, we will briefly comment on it in the discussion.

Out of the three descriptors required for the qualitative level, the dipole moment and the polarizability possess clear-cut definitions, whereas the excluded volume represents a more vague term. Here, the goal is to develop excluded volume descriptors useful for analyzing trends both qualitatively and quantitatively, and that may also point the way to reducing the number of free parameters in one-electron model Hamiltonians for non-valence-bound states.

To this end, first the new class of dipole-bound electrons to amine N-oxides is investigated so as to establish a consistent data set of electron binding energies and properties. Amine N-oxides were chosen for three reasons: First, owing to their very polar coordinate covalent NO bond, they possess high dipole moments. Second, the three substituents on the N atom directly control the excluded volumes. Third, dipole-bound states of amine N-oxides have not been systematically studied, and thus the data set alone represents a significant finding.

Then, various excluded volume descriptors are defined, evaluated, and accessed regarding their use in the qualitative comparison of certain isomer groups as well as their use as quantitative descriptors in qualitative structure-property relationships (QSPR) for the whole data set.

II. COMPUTATIONAL METHODS

A. Excluded Volume Descriptors

While giving a qualitative description of an excluded volume is fairly straightforward (see the Introduction), giving a quantitative definition is less straightforward. Let us at this point

emphasize that the excluded-volume as understood in the context of dipole-bound anions is quite different from the excluded-volume used in the theory of liquids and gases. Both are "crowding effects", however, while in solution and gases the whole molecular volume of molecule A is unavailable to molecule B, in the context of dipole-bound states the question pertains to groups or molecules excluding the excess electron from approaching the positive center of the dipole.

To compute the excluded-volume in dipole-bound states, it is thus insufficient to know the volume of the crowing groups or cluster members. Instead an integral is needed, which weighs volume closer to the positive center and volume in the direction of the dipole vector more heavily, and the type of atoms in the volume to be integrated over make little difference.

All descriptors defined below rely on the identification of a "positive center", $\vec{R}_+$, and are therefore most easily applicable to the special case of a molecule possessing a single strongly polar group from which the molecular dipole derives. As chemical intuition suggests, and Löwdin or Mullikan populations confirm, for amine N-oxides the choice $\vec{R}_+ = \vec{R}_N$ is well-justified.

Other obvious examples with a fairly obvious choice of $\vec{R}_+$ are organic molecules that feature only a single nitrile or nitro group, although for these two compound classes the precise location of $\vec{R}_+$ becomes less clear if the polar group is attached to a conjugated π-system. Further generalizations are obviously needed for molecules with various binding sites, say, water clusters with multiple dangling OH bonds.

While a more general definition of our excluded volume descriptors is in principle possible, the definitions for a single positive center are attractive due to their simplicity, their small number of parameters, and their suitability for the present context. Therefore, for this pilot application, we restrict ourselves to simple models.

A first descriptor for the excluded volume is based on a density for the excess electron $\rho(\vec{r})$ and measures directly how close the excess electron can approach the positive center:

$$\langle r_+ \rangle = \int d^3r \ \mid \vec{r} - \vec{R}_+ \mid \ \rho(\vec{r}) \tag{1}$$

Possible choices for $\rho(\vec{r})$ are the lowest unoccupied orbital (LUMO) of a Hartree-Fock calculation for the neutral, the singly occupied orbital of a Hartree-Fock calculation for the anion, or natural or Dyson orbitals from direct methods to compute the electron attachment energy such as EA-EOM-CCSD or ADC[22].

Yet, the descriptor $\langle r_+ \rangle$ possesses—by construction—two great disadvantages. First, any descriptor based on $\rho(\vec{r})$ is, of course, unsatisfactory in that it implies finding the density of the anion first. Indeed, $\langle r_+ \rangle$ tastes and feels more like an analysis approach for the electronic structure of anions than a qualitative descriptor of the neutral. Second, while $\langle r_+ \rangle$ reflects without any doubt the effects of any substituent that prevents the excess electrons from approaching the positive center, it also reflects any other influence on the electron distribution, say, that of the dipole moment. Therefore $\langle r_+ \rangle$ can only serve as an indirect descriptor for the excluded volume; it may, however, serve as a general descriptor of a dipole-bound state and aid in interpreting electron distributions of non-valence states (c.f. Ref. [23]).

More direct descriptors for the excluded volume can be defined by integrating the van der Waals volume of the neutral molecule from the positive center in the direction of the dipole. To compute these descriptors, $V_x^{(i)}$, one needs four ingredients: the position of the nuclei to define the van der Waals volume, the position of the positive center $\vec{R}_+$ (here, the position of the N atom), the direction of the dipole $\vec{\mu}$ (here, the direction of the N-O bond), and, last, a weight function, w_i that picks out the part of the molecule hindering the excess electron to approach $\vec{R}_+$

$$V_x^{(i)} = \int_{V_{vdW}} d^3r \, w_i(\cos\theta, \, r_+) \tag{2}$$

Here the integral is evaluated over the van der Waals volume of the neutral (see ref. [24] for radii), and $w_i(r_+, \cos\theta)$ is one of three weight functions defined below, which depend on the distance from the positive center r_+ and the angle θ between the dipole vector and the vector from the positive center to the position of the electron $\vec{r}$:

$$r_+ = \mid \vec{r} - \vec{R}_+ \mid \qquad \cos\theta = \frac{\vec{\mu} \cdot (\vec{r} - \vec{R}_+)}{\mu r_+} \tag{3}$$

The first weight function $w_1(\cos\theta)$ simply integrates all volume in the direction of the dipole vector and goes to zero for $\theta = 90°$, but does not discriminate for distance:

$$w_1(\theta) = \begin{cases} \cos\theta \; : \; \cos\theta > 0 \\ 0 \quad : \quad \text{else} \end{cases} \tag{4}$$

Alternative definitions are motivated by *ab initio* and model electron densities of dipole bound states, which show maxima close to the positive center and then fall off suggesting

that the weight function should also fall off with r_+. Two models were considered:

$$w_2(\theta, r_+) = \begin{cases} \cos\theta \, r_+^2 \, e^{-r_+/r_0} & : \cos\theta > 0 \\ 0 & : \text{else} \end{cases} \tag{5}$$

and

$$w_3(\theta, r_+) = \begin{cases} \cos\theta \, r_+^2 \, e^{-r_+^2/r_0^2} & : \cos\theta > 0 \\ 0 & : \text{else} \end{cases} \tag{6}$$

Both weight functions w_2 and w_3 rise quadratically from the origin, show a maximum, and fall off to zero, and for both the parameter r_0 is chosen such that the maximum occurs at the van der Waals radius of an N atom (1.55 Å[24]).

The absolute excluded volumes computed by these means are more or less arbitrary; what matters are the relative values used to compare different N-amine oxides. We therefore express all excluded volumes relative to a reference value, and choose $V_x^{(i)}$ of H_3NO for this purpose. Thus, regardless of weight function, the excluded volume of H_3NO is defined to be 1, and trends obtained with different weights can be compared in a meaningful way.

B. *Ab initio* Methods

The following computational protocol has been used to establish the data set comprising electron binding energies and properties: First, the geometry of the neutral amine-N-oxide was optimized using second-order Møller-Plesset perturbation theory (MP2) and the jul-cc-pVTZ basis set[25,26]. The same basis set was used to compute self-consistent-field (SCF) and MP2 dipole moments as well as SCF and MP2 polarizabilities.

Dipole-bound states of molecules normally show only a very small geometry relaxation upon electron attachment, and the vertical electron affinity of the respective neutral, the vertical electron detachment energy of the anion, and the adiabatic electron affinity typically vary by less than 5%. [In contrast, dipole-bound states of clusters, show often substantial geometry changes, the water dimer is a drastic example[4].] Therefore, only the vertical electron affinity of the neutral was computed, and we refer to it as binding energy, E_b.

In all calculations of the binding energy, the aug-cc-pVDZ basis[25] was augmented with several further sets of diffuse s, p, and d functions centered on the amine N atom, which represents the positive center of the molecular dipole (see ref.[9,27] for basis set requirements of dipole-bound states). The exponents of these functions were chosen as an even-tempered

series starting from the respective smallest exponent in the nitrogen aug-cc-pVDZ set with a scaling factor of 3.5. The number of additional spd sets needed to converge the computed binding energies depends on the specific amine N-oxide and the theoretical method employed. In most cases a (5s5p5d) set yields well-converged results, and all results reported here were obtained with at least this set. However, some low-binders require up to (7s7p7d) to converge the uncorrelated Koopmans's Theorem (KT) estimate of E_b.

Apart from KT, E_b was computed with so called Δ-methods, where E_b is obtained as the difference between the total energies of the neutral and the anion as well as with so-called direct methods, which avoid computing an explicit anion wavefunction and yield E_b directly. Initially many Δ-methods and direct methods were compared for the two smallest systems and the less costly methods were further compared for two typical intermediate-size amine N-oxides.

The particuar Δ-methods used in this study were ΔSCF, ΔMP2, ΔOO-MP2 (orbital optimized MP2), and the Δ coupled-cluster variants ΔCCSD, ΔCCSD(T), ΔCCSDT, ΔCCSDT(Q), that is, up to Δ-coupled cluster with iterative single, double, and triple substitutions and non-iterative quadruple substitutions. For all Δ-methods spin-unrestricted SCF calculations were used to compute the energy of the anion, and, as expected for dipole-bound states, spin contamination is negligible.

All direct methods beyond KT were variants of the equation-of-motion (EOM) coupled-cluster family[28,29]: EOM-CCSD, its second-order approximation EOM-CCSD(2), which is sometimes referred to as EOM-MP2, EOM-CCSDT, as well as three different corrections of EOM-CCSD for triple substitutions: EOM-CCSD*, EOM-CCSD(T)(a)*, and EOM-CCSD(T)(a) (see the discussion in Ref. [29] for details).

Four *ab initio* codes were used. The Orca package[30,31] (version 4.1) was used for optimizations, to compute dipoles, polarizabilities as well as OO-MP2 and many EOM-CCSD calculations. However, geometry optimizations with confined dihedral angles were carried out using the Psi4 package, version 1.2[32]. Further EOM-CCSD calculations, in particular for natural orbitals, as well as all other EOM calculations were carried out with version 2.1 of the CFOUR package[33]. Last, CCSDT, CCSDT[Q], and CCSDT(Q) calculations were carried out through the MRCC[34] interface provided by CFOUR.

III. RESULTS AND DISCUSSION

In this section we will first report and discuss *ab initio* results and excluded volume descriptors for all amine N-oxides studied. Then, we will compare particular sets of isomers, conformers, or conformations that show excluded volume influences most clearly, before discussing how the descriptors can be used in QSRP models of the binding energy.

Sixteen different amine N-oxides were investigated (see Tab. I); eleven of these have just one relevant conformer, yet, ethylamine N-oxide, isopropylamine N-oxide, and piperidine N-oxide possess two, ethylmethylamine N-oxide possesses three, and propylamine N-oxide possesses four. Moreover, we include the synperiplanar (syn) conformation of ethylamine N-oxide (torsion angle of 0.0° between the NO and the CC bonds) making a total of 25 dipole-bound states. Cartesian coordinates of all considered structures are available as supplementary information.

A. Correlation Effects on the Binding Energy of Dipole-bound States

Predicting accurate electron binding energies represents one of the more challenging tasks of quantum chemistry. Well known issues include the more diffuse nature of anions, lack of error compensation due to the neutral and anion possessing a different number of electrons (methods must be size extensive), and, in case of density functional calculations, the need for the correct behavior of the self-interaction energy[2,35]. Our molecule set includes some fairly large amine N-oxides, and it was clear that we could not afford to compute highly accurate E_b values for the larger species. Nevertheless, in order to establish a consistent data set, we needed an affordable yet sufficiently accurate method. Hence, the two smallest amine N-oxides were studied with very accurate methods, and two intermediate-size systems were studied with some of the more costly methods.

Our results are collected in Tab. II. The rough trends emerging for the N-oxides follow the typical trends that were initially established in Refs. [10,11] and summarized in Refs [2,4,9]: Relative to a purely electrostatic picture (no electron correlation) as defined by the KT binding energy, electron correlation increases E_b dramatically. In contrast, average orbital relaxation as described by a ΔSCF calculation has virtually no impact on E_b.

In view of being the most primitive correlated level, ΔMP2 represents a big improvement

over KT, but to capture a substantial share of the correlation contribution to E_b, at the very least an ΔOO-MP2 or an EOM-CCSD(2) calculation is needed. For many other dipole-bound or other non-valence anions, even that may be insufficient for acceptable accuracy[6], but for the large-dipole low-polarizability amine N-oxides considered here, these two second-order methods are very competitive. As discussed in Ref. [6], the critical ingredient for a reliable method is its ability to account for orbital relaxation in the presence of electron correlation, and both orbital-optimized MP2 as well as equation-of-motion methods share this feature.

Correlation effects beyond EOM-CCSD can be investigated in two ways. First, the EOM-CCSD energy can be corrected for triple substitutions. The four molecules considered in Tab. II demonstrate that the absolute effects are only a few meV, but the relative changes are increases in E_b of about 5%.

Second, the EOM-CCSD value can be compared with Δ-methods, but owing to the totally different theoretical approaches, it is not so clear which Δ-method compares most directly to EOM-CCSD itself. What is clear, however, is that ΔCCSD captures very roughly 90% of the binding energy, and that ΔCCSDT seems converged as judged by additional changes of perturbative quadruple substitutions, but slightly too small in comparison to EOM-CCSDT. The so called golden standard, ΔCCSD(T), yields somewhat smaller binding energies than ΔCCSDT, and in contrast to many "closed-shell-only properties," CCSD(T) seems inferior to the full triples method in the present context—presumably owing to the lack of error compensation typically associated with calculating electron binding energies.

Based on the results in Tab. II, we decided on EOM-CCSD as a workhorse method, because we were able to do EOM-CCSD calculations for all but one amine N-oxide, and because the accuracy of EOM-CCSD(2) can be expected to deteriorate for the high polarizability, low E_b cases[6]. Moreover, E_b was computed for all molecules using KT to provide an electrostatic reference and using ΔOO-MP2 as the best tradeoff between accuracy and affordability.

B. *Ab Initio* Results and Excluded Volume Descriptors

For every amine N-oxide considered, Tab. III reports the electron binding energy computed with KT, EOM-CCSD, and ΔOO-MP2, the dipole moment μ, the polarizability α,

and the excluded volume descriptors defined in eq.(1) and eq.(2).

Before trying to identify any specific relationship, let us discuss a few general trends in the established data set:

1. Similar to the four amine N-oxides discussed in depth in the last subsection, the electrostatic value for E_b obtained using KT is always substantially lower than the many-body result obtained using EOM-CCSD or ΔOO-MP2.

2. The EOM-CCSD binding energies range from just shy of 20 meV to about 60 meV with the single exception of H_3NO, which shows an E_b of 121.4 meV—more than twice as large as the next smaller E_b.

3. The MP2 dipole moments range from 4 to 6 D, and the SCF values are only slightly larger than the MP2 dipoles (differences of 0.18 to 0.08 D, which is less than 5%). Clearly, the relaxation of the electron density due to many-body effects is small, and SCF dipoles are a good approximation for this molecule class.

4. Similar to the dipole moments, the SCF and MP2 polarizabilities agree well (to about 3%) with each other. However, in contrast to the dipole predictions, the two values correlate perfectly with each other (coefficient of determination of 1.0) and almost perfectly with the molar mass (coefficient of determination of 0.999).

5. The excluded volume values, $V_x^{(i)}$, from our models (eq.(2)) display surprisingly little "group additivity," even when considering very simple series such as, say, H_3NO, MeH_2NO, Me_2HNO, Me_3NO or H_3NO, PhH_2NO, Ph_2HNO, Ph_3NO, and the same is true for $\langle r_+ \rangle$.

6. The differences in the $\langle r_+ \rangle$ values derived from SCF LUMOs and EOM-CCSD natural orbitals reflect the difference in the E_b values predicted by KT and EOM-CCSD.

The next question is whether—or to what extent—any of the computed parameters can explain the trends of the binding energies. Fig. 1 investigates this question by plotting the binding energy vs. the dipole moment, the polarizability, and selected excluded volume descriptors.

All four plots show some degree of correlation—the dipole moment a positive one, and the three other parameters a negative one—but even by-eye it is obvious that only $\langle r_+ \rangle$ shows a

semi-acceptable correlation with E_b. As discussed above, any E_b vs. $\langle r_+ \rangle$ correlation is not much of a surprise, since both quantities originate from closely related *ab initio* calculations. On the contrary, we find it rather astounding that this correlation is not significantly better.

More astounding, in a class of closely related *dipole-bound* anions with dipoles varying over a wide range of 2 D, one should expect a clear correlation of the binding energy with the dipole moment, but even ignoring H_3NO, the E_b vs. μ correlation is obviously poor. We therefore conclude that the trends in the binding energy cannot be explained by a single parameter, but that several parameters have to be combined.

One way to identify at least qualitative trends consists of comparing the isomers and groups and conformers having the same molar mass. By this means, polarizability can be effectively eliminated as a variable, as the involved polarizabilities are almost equal, and the trends for this specific subgroup can be studied in terms of the dipoles and the excluded volume alone. The first group of amine N-oxides that can be compared in this way is the C_2H_7NO group, which consists of Me_2HNO and EtH_2NO. We first consider the different EtH_2NO conformations in some detail before comparing them with their Me_2HNO isomer. Then we discuss the $C_3H_{10}NO$ group.

EtH_2NO possesses two conformers, anti and gauche, and its conformational space can be studied by varying a single variable: the O–N–C–C torsion angle θ. We studied the behavior along this coordinate by keeping this angle frozen at 13 different values, optimizing the geometry of all other structural parameters, and computing E_b, μ, and $V_x^{(i)}$ for each optimized structure (Fig. 2).

The binding energy is essentially flat (46 – 49 meV), showing only a small oscillation with the 120° frequency that is typically associated with the changes between eclipsed and staggered conformations. In contrast, both the dipole and the excluded volume descriptors display sigmoid character. The dipole increases from about 5 D to 5.7 D, and the excluded volume descriptors increase almost synchronously with it. However, while $V_x^{(1)}$ and $V_x^{(2)}$ approximately double, $V_x^{(3)}$ increases "only" by 25%. Be that as it may, the major trend of a binding energy, which is essentially independent of torsion angle, can only be explained by considering both, μ and V_x, and the impacts of the two must practically cancel each other out.

A visual impression of the excluded volume effect can be gained from cuts through the "singly occupied" EOM-CCSD natural orbitals (occupation numbers of 0.998), which de-

scribe the dipole-bound electron (Fig. 3). For both the syn and the anti conformation, the electron distribution resembles a large s-type orbital off the dipole created by the NO group. Loosely speaking, both electron distributions look like apples, with two stems: the N–O bond, and the N-ethyl chain. The NO bond creates the dipole and points more of less towards the apple core. In contrast, for the syn conformation, the ethyl group bends back from the electron density (the apple) and may influence it only via long range forces. while, for the anti conformer, the ethyl group points directly into the electron density; in the apple picture, the ethyl-stem bents back and punches a hole into the core.

While the natural orbitals offer an intuitive understanding of the excluded volume, they unfortunately offer little understanding of why the smooth synchronous increases of both dipole moment and excluded volume lead to such small variations in binding energy.

The second member of the molar mass C_2H_7NO group, Me_2HNO, possesses only one stable conformation, and only this structure is considered. The electron binding energy of this Me_2HNO structure is considerably smaller than that of EtH_2NO regardless of the torsion angle of the latter, and the question is, Why? Since the dipole and excluded volume of EtH_2NO are torsion dependent, the most direct comparison of Me_2HNO and EtH_2NO involves lining up either the dipole or the excluded volume. In order to compare identical dipoles, EtH_2NO conformations with $\theta < 50^\circ$ must be considered. These EtH_2NO structures show a substantially smaller excluded volume than Me_2HNO, explaining the lower E_b of Me_2HNO. Conversely, if structures of identical excluded volume are to be compared, it turns out that Me_2HNO should be compared with EtH_2NO conformations close to $\theta \approx 180^\circ$, which show a substantially higher dipole moment than Me_2HNO, and again the E_b trend is easily explained.

The $C_3H_{10}NO$ group contains Me_3NO, two $iPrH_2NO$ conformers, three EtMeHNO conformers, and four $nPrH_2NO$ conformers. Similar to the C_2H_7NO group, the polarizabilities of these 10 structures are very similar, and the binding energy should depend primarily on two variables only: the dipole moment and the excluded volume. The particular dependency on μ and $V_x^{(2)}$ is shown in Fig. (4). Apart from a change in scale, the analogous figure based on $V_x^{(1)}$ looks practically identical. Using $V_x^{(3)}$, on the other hand, yields a somewhat different pattern; however, the conclusion reached is identical.

In the $C_3H_{10}NO$ group, the highest binding energies are associated with the lowest excluded volumes and fairly small dipole moments (lower left corner of Fig. (4)). If one then

keeps the dipole fixed at about 5 D and increases V_x, the binding energy drops accordingly, emphasizing again the excluded volume effect and that the definition of our descriptor makes at least qualitative sense (left edge of Fig. (4)). However, if both μ and V_x are changed at the same time, no clear pattern emerges. At best, one can say that along the diagonal of Fig. (4), the binding energy shows no clear trend, but that the variations are also smaller than in the lower left corner of Fig. (4). Therefore, similar to the EtH_2NO conformation, the increasing dipole moment and excluded volume must largely cancel each other out. While a straightforward quantitative trend may not be obvious (at least not to us), it seems obvious that dipole moment and excluded volume both represent significant but opposing influences on the binding energy.

C. Empirical Models for the Binding Energy

Having discussed trends in the binding energies of isomer groups in the light of our excluded volume descriptors, this section explores the utility of the descriptors as quantitative parameters in QSPR of the binding energy. The mathematical form of these relationships separates the effects of the dipole moment μ, the excluded volume V_x, and the polarizability α and is motivated partly by the careful analysis of one-electron model Hamiltonians[14], partly by our own empirical observations, and partly by the separation of the binding energy into two contributions, one due to electrostatic one due to electron correlation effects[4,10].

One-particle model Hamiltonians describing a light charged particle bound to a dipole have been developed by many groups (see e.g.[12,14,36,37]). As a rule, the model potentials display cylinder symmetry, but nevertheless separate into an angular and a radial equation in spherical coordinates. While the exact solution of these equations requires numerical steps, for certain simple models approximate closed-form solutions can be obtained. One such model potential consists of a point-dipole and a hard sphere repulsive shell[14]. In this model the binding energy is approximately

$$E_b \cong A\frac{e^{-B/\sqrt{\mu-\mu_0}+C\sqrt{\mu-\mu_0}}}{r_s^2} \tag{7}$$

where μ_0 is the critical dipole moment of 1.625 D, r_s is the radius of the hard-sphere repulsive core, and A, B and C are three parameters: A is a proportionality constant, the B term is the leading term describing the threshold behavior, and the C term is the first correction.

While A, B and C can in principle be derived from analytic expressions, the authors of Ref. [14] treat them as fitting parameters and found that eq.(7) almost perfectly reproduces the exact (numerical) solutions of their model.

We note that the analysis in Ref. [14] initially meanders towards a primitive representation of an excluded volume in terms of the parameter r_s, which can be computed for any molecule provided μ and E_b are known: $r_s(E_b, \mu)$. However, the r_s values computed by these means were deemed "nonphysical," and the model Hamiltonian was then extended by a polarization potential featuring an additional polarizability dependent cutoff radius, chosen so as to render r_s a system-independent constant.

Be this as it may, the analytical expression for E_b (eq.(7)) immediately suggests replacing r_s with $V_x^{(i)}$, and we consider the following two simple QSPRs:

$$E_b = A\frac{e^{-B/\sqrt{\mu-\mu_0}}}{{V_x^{(i)}}^m} \tag{8}$$

and

$$E_b = A\frac{e^{-B/\sqrt{\mu-\mu_0}+C\sqrt{\mu-\mu_0}}}{{V_x^{(i)}}^m} \tag{9}$$

where the exponent m of $V_x^{(i)}$ is an additional fit parameter that would be 2/3 if the excluded volume was spherical and the analytical expression from Ref. [14] was exactly valid. Since both QSPRs do not include the polarizability, it is natural to use eqs.(8) and (9) to fit the KT values for E_b, and to include electron correlation effects at a second stage.

A third QSPR considered is based on our empirical observation that in a log-log plot electron binding energies of dipole-bound states show a roughly linear correlation with the dipole moment (needless to say, this correlation shows a lot of noise and its application is limited to "lines that guide the eye"). Still, a power law for the dipole dependence of the binding energy may be a reasonable model, and as a second three-parameter model we study

$$E_b = A\frac{(\mu-\mu_0)^n}{{V_x^{(i)}}^m} \tag{10}$$

Again, this relationship lacks any dependency on the polarizability, and is therefore fitted to KT binding energies.

Results from fitting the three QSPRs defined in eqs.(8), (9) and (10) are collected in Tab. IV. Each of the three relationships is fitted in combination with each of the three excluded volume descriptors $V_x^{(i)}$ yielding a total of nine parameter sets. Regarding opti-

mization of parameters, we minimized the mean square error based on relative errors

$$\chi^2 = \frac{1}{N} \sum \left(\frac{E_b^{KT} - E_b^{model}}{E_b^{KT}} \right)^2 \tag{11}$$

Relative errors are needed for this purpose because the electron binding energy of H_3NO represents a brutal outlier that would dominate χ^2 otherwise. However, for the purpose of comparing different model/excluded-volume-descriptor combinations, we do not use χ^2, but rather the mean of the absolute value of the relative errors (MARE)

$$MARE = \frac{1}{N} \sum \frac{\mid E_b^{KT} - E_b^{model} \mid}{E_b^{KT}} \tag{12}$$

because it has the same unit as the relative error and is the more intuitive quantity.

For all nine QSPR/excluded-volume-descriptor combinations, the MARE fall in the range between 7% and 15%. While these errors may seem large, they should be seen in the context of the simplicity of the three QSPRs and the obvious lack of any direct correlation of E_b with either μ or V_x.

The main MARE differences are due to the excluded volume descriptors with $V_x^{(2)}$ performing best, $V_x^{(1)}$ being a very close runner-up, and $V_x^{(3)}$ performing significantly worse. However, we note that both $V_x^{(2)}$ and $V_x^{(3)}$ depend on a length-scale parameter that has been arbitrarily chosen to reflect the size of an N atom. An optimization of this parameter will, of course, result in a smaller MARE, the question is only whether the gain is worth introducing yet another free parameter. At this point our data set seems too small to explore this question.

In contrast to the different excluded volume descriptors, the three QSPRs perform at a very similar level. While the second model (eq.(9)) must by definition outperform the first (eq.(8)), introducing the C parameter does not significantly improve the description of the data. Similarly, only slight differences between the performance of the first and the third model can be observed for a given excluded volume descriptor.

In addition to the similar performance of the three QSPRs, note the following consistencies in the optimized parameters: (1) The exponent m of the excluded volume depends only on the excluded volume descriptor, but is virtually independent of the QSPR. (2) The exponents associated with $V_x^{(1)}$ and $V_x^{(2)}$ are roughly 0.85 ± 0.02 and 0.77 ± 0.02, so $V_x^{(1)}$ and $V_x^{(2)}$ indeed behave similar to a hard-sphere volume ($m = 2/3$). (3) The exponent of the dipole moment, n, in the empirical model (eq.(10)) is fairly close to 4. Thus, at least a

posteriori it seems possible to reduce the number of free parameters by replacing a subset (n and m are obvious candidates) with fixed integers or fractions, e.g., for $V_x^{(2)}$: $n = 4$ and $m = 3/4$.

Last, we turn to the correlation contribution to electron binding energy

$$E_{corr}^{abs} = E_b - E_{KT} \tag{13}$$

In order to create a consistent data set for all amine N-oxides, E_b is estimated using OO-MP2. Naively, one might expect that E_{corr}^{abs} should correlate with polarizability, perhaps even in a linear fashion. Yet, this is clearly not so: the lightest molecule, H_3NO, possesses the smallest polarizability, but it shows by far the largest E_{corr}^{abs}. Indeed, as surprising as this may seem, a plot of E_{corr}^{abs} *vs.* α suggests that E_{corr}^{abs} and α are in fact uncorrelated.

On the other hand, one-electron model Hamiltonians demonstrate that a wide range of data can be reproduced by point-dipole and point-polarizable site models (see e.g.[14,37,38]). Hence, one is led to the conclusion that electrostatics and polarizability do not act independently but rather cooperatively. In an *ab initio* context, which separates E_b into KT and rest, we unfortunately cannot directly account for cooperation, however, we can switch to a definition of the correlation contribution in relative terms:

$$E_{corr} = E_{corr}^{rel} = \frac{E_b - E_{KT}}{E_b} \cdot 100\% \tag{14}$$

At least for the present data set the relative correlation energy E_{corr} generally grows with molecular polarizability and for the highest polarizabilities—by construction—shows a saturation close to 100%.

The definition of E_{corr} as a relative quantity has two further advantages. First, the overall shape of an $E_{corr}(\alpha)$ model can be adumbrated from its asymptotics: For vanishing α, E_{corr} must approach zero, and for large α, E_{corr} must approach 100%, and thus $E_{corr}(\alpha)$ must behave like a switching or sigmoid function. Second, eq.(14) naturally includes correlation-bound states, which do not bind at KT, and normally show only relatively small binding energies, but large polarizabilities.

One strategy is then to fit the data with one of the well known sigmoid functions from the literature, say,

$$E_{corr} = \frac{200}{\pi} \arctan \frac{\pi}{2} b\alpha \tag{15}$$

where b is a free scaling parameter. This straightforward one-parameter function fulfills the conditions for $\alpha = 0$ and $\alpha \to \infty$ and yields a very satisfactory fit with a MARE of 4.4%. The fit can be improved by three means: First, a sigmoid function with more free parameters, such as the general logistic function

$$E_{corr} = \frac{100}{(1 + Qe^{-b\alpha})^{\frac{1}{n}}} \tag{16}$$

may be chosen, where Q, b and n are free parameters. Second, the condition $E_{corr}(0) = 0$ may be relaxed so as to fit only in the given domain of polarizabilities, in particular, because the threshold law of $E_{corr}(\alpha)$ is unknown. Third, after making the first two improvements, the fit can be further enhanced by replacing the isotropic polarizability, which has so far been tacitly used, by $\alpha_\perp$, the average polarizability perpendicular to the direction of the dipole vector. [It goes without saying that replacing α with the parallel component, $\alpha_\parallel$, yields a correspondingly worse fit.] Still, implementing all three improvements brings the MARE down by only 1.5% and the best fits that can be obtained in this way show MAREs in the order of 2.9%. The two optimized switching functions (eq.(15) and eq.(16)) are compared in Fig.5.

IV. SUMMARY AND CONCLUSIONS

Trends in electron binding energies of dipole-bound states can be understood in terms of three properties of the neutral molecule: Its dipole moment, μ, its polarizability, α and its excluded volume, V_x, which is any volume close to the positive end of the dipole, a dipole-bound electron is crowded out of by unpolar substituents or other molecules[3,19]. All three, μ, α, and V_x are also used in one-electron models for dipole-bound states, however, while the dipole moment and the polarizability are well-defined quantities, V_x is not.

Here, we aim at developing descriptors for the excluded volume that are useful for analyzing trends qualitatively and quantitatively and that may also point the way toward a reduction of the number of free parameters in general one-electron model Hamiltonians for non-valence-bound states.

To this end, first a data set comprising electron binding energies and properties of 25 amine N-oxides is established. Amine N-oxides were chosen because they possess high moments on account of their very polar NO bond, and their excluded volume can be easily

controlled by varying the three substituents on the N atom. Moreover, dipole-bound states of amine N-oxides have not been systematically studied, and thus the data set alone represents a significant finding. Specifically, the electron binding energy, E_b, the dipole moment and the polarizability are computed at the one-particle and the many-particle level.

Next, various descriptors for V_x are defined (see eqs.(1) and (2)). Two descriptors depend on the density of the excess electron. These are—by construction—less useful, because, on the one hand, a reliable, and therefore computationally expensive density must be computed first, and, on the other hand, the electron density itself is influenced by μ, α, and V_x, and isolating the V_x influence is anything but straightforward. In contrast, the three definitions in eq.(2) are functions of the molecular structure and the direction of the dipole moment only, any prior computation of the anion state is unnecessary, and computing V_x is computationally inexpensive.

The benefit of the excluded volume descriptors $V_x^{(n)}$ $(n = 1 - 3)$ defined in eq.(2) was demonstrated in a systematic comparison of sets of isomers, conformers and conformations. These subsets of amine N-oxides possess identical molar masses and therefore almost identical polarizabilities, and regarding the present context, their differences in E_b should thus be due to their differences in dipole and excluded volume. For all subsets considered in this way, even including sets that just contained conformations of a single isomer, it turned out that the trends in E_b could only be explained by a combination of μ and V_x, but not by either factor on its own.

Our findings at the qualitative level are clearly reflected in the simple QSPRs developed to predict the electrostatic part of the binding energy as function of μ and V_x (eqs.(8) – (10)). The most direct comparison of the impacts of μ and V_x is perhaps possible for the empirical model (eq.(10)) and $V_x^{(2)}$: In this QSPR/$\mathrm{V}_x^{(i)}$ combination the exponent of $(\mu - \mu_0)$ is close to 4 and the exponent of V_x is close to $-3/4$, and therefore one might think that variations in dipole moment have a larger impact on the binding energy. While this is true from a strict mathematical point of view, the typical ranges invert the picture: Dipoles vary only from 4 to 6 D (150%), whereas $V_x^{(2)}$ varies from 1 to 17, and thus the smaller exponent of $V_x^{(2)}$ is easily over-compensated by its range of values, giving the excluded volume—at least for this class of molecules—a somewhat larger impact on the binding energy.

Further, let us note that combinations of any of the three QSPRs with either $V_x^{(1)}$ or $V_x^{(2)}$ fit the *ab initio* data reasonably well (MAREs in the order of magnitude of $7 - 8\%$). This is

quite remarkable because the electron-molecule interactions in dipole-bound states are weak and subject to subtle effects, and while the dipole and excluded volume may dominate the long and short-range interactions, respectively, there will be various higher-order and cross terms that become important at intermediate ranges.

Fitting in a second step E_{corr} suggests the following interpretation: Starting from the electrostatic contribution to the electron-molecule interaction, which is determined by the dipole moment and the excluded volume, the correlation contribution is determined by the molecular polarizability. However, electrostatics and polarizability act cooperatively, and hence only the relative correlation contribution to the binding energy (eq.(14)) can be related to polarizability, where the functional form $E_{corr}(\alpha)$ must follow a sigmoid function.

A fit of E_{corr} can be slightly improved by using the polarizability component perpendicular to the dipole vector, $\alpha_{\perp}$, as a dependent variable, suggesting that while the polarizability can be thought of as contracting the electron density in all directions, the direction orthogonal to the dipole axis is somewhat more important than the direction of the dipole itself. Only a slight improvement, but nonetheless one that demonstrates that even simple fitting procedures can sometimes offer a glimpse of physical insight.

Our best QSPR of E_{corr} features a MARE of less than 3%, which is highly competitive in view of the high computational cost of obtaining a reliable E_{corr} in *ab initio* calculations. Thus, our results suggest that—at least for a family of closely related compounds—an accurate electron binding energy can be predicted from the dipole moment, the polarizability, one of our excluded volume descriptors, and the KT value of the binding energy.

Last, let us briefly comment on the recent measurements by Castellani *et. al.*[21]. In summary, Liu *et. al.*[39] measured the binding energy of the non-valence anion state of phenoxide (Ph-O), which is 12 meV. In Ref. [21], spectra of various para-substituted phenoxides were compared with Ph-O itself, and it was demonstrated that this non-valence state is "not destroyed" by alkyl substitution; however, the binding energy itself was not reported.

We emphasize that the following is conjecture, because, in the first place, the particular values of the binding energies with increrasing alkyl group length are unknown. In the second place, while the dipole-moments of the phenoxides are predicted to be about 4 D[21,39] and therefore comparable to the smallest dipoles in the N-amine oxide class, the observed binding energy of 12 meV is considerably smaller than that of any N-amine oxide energies.

The most direct comparison can perhaps be made between Ph-O and Ph_3NO, because

both possess similar dipole moments and Ph_3NO possesses the smallest E_b in our data set. Another option may be $PhMe_2NO$, which may provide a closer match in excluded volume (the excluded volume of Ph-O cannot be defined in as simple terms as the one for N-amine oxides, since the positive center is at least to some extent delocalized over the ring). Nonetheless, for both Ph_3NO and $PhMe_2NO$ the lion's share of the binding energy stems from electron correlation, which together with the small binding energy of 12 meV suggests that the non-valence state of Ph-O has significant polarization-bound character.

Based on this scant information, we put forward two possible explanations for the experimental observations: First, provided the electrostatic contribution to the binding energy of a non-valence state is small, the excluded volume will have only a minor impact on the total binding energy, because it affects only the former (the KT part for the N-amine oxides). Second, the impact of alkyl substitution on the electrostatic part of the binding energy may be compensated by an increase in polarizability, in particular, if the electrostatic contribution is small. In-depth experimental or theoretical studies are needed to shed light on this fundamental issue.

SUPPLEMENTARY MATERIAL

See supplementary material for the optimized structures of all N-amine oxides considered.

ACKNOWLEDGMENTS

The author greatly appreciates fruitful discussions with Kenneth D. Jordan. Support by the National Science Foundation under CHE-1565495 is gratefully acknowledged.

REFERENCES

[1] J. Simons, J. Phys. Chem. A **112**, 6401 (2008).

[2] J. Simons, Ann. Rev. Phys. Chem. **62**, 107 (2011).

[3] N. I. Hammer, K. Diri, K. D. Jordan, C. Desfrancois, and R. N. Compton, J. Chem. Phys. **119**, 3650 (2003).

[4] K. D. Jordan and F. Wang, Annu. Rev. Phys. Chem. **54**, 367 (2003).

[5]T. Sommerfeld, B. Bhattarai, V. P. Vysotskiy, and L. S. Cederbaum, J. Chem. Phys. **133**, 114301 (2010).

[6]V. K. Voora, A. Kairalapova, T. Sommerfeld, and K. D. Jordan, J. Chem. Phys. **147**, 214114 (2017).

[7]J. Kalcher, P. Rosmus, and M. Quack, Can. J. Phys. **62**, 1323 (1983).

[8]J. V. Ortiz, J. Chem. Phys. **87**, 3557 (1987).

[9]J. M. Herbert, in *Reviews in Computational Chemistry*, Vol. 28, edited by A. L. Parrill and K. B. Lipkowitz (John Wiley & Sons, Hoboken, NJ, USA, 2015) pp. 391–517.

[10]M. Gutowski, P. Skurski, A. I. Boldyrev, J. Simons, and K. D. Jordan, Phys. Rev. A **54**, 1906 (1996).

[11]M. Gutowski, P. Skurski, K. D. Jordan, and J. Simons, Int. J. Quant. Chem. **64**, 183 (1997).

[12]D. C. Clary, J. Phys. Chem. **92**, 3173 (1988).

[13]C. Desfrançois, Phys. Rev. A **51**, 3667 (1995).

[14]G. F. Gribakin and A. R. Swann, J. Phys. B **48**, 215101 (2015).

[15]T. Sommerfeld, A. DeFusco, and K. D. Jordan, J. Phys. Chem. A **112**, 11021 (2008).

[16]L. Turi and P. J. Rossky, Chem. Rev. **112**, 5641 (2012).

[17]L. Mones, P. J. Rossky, and L. Turi, J. Chem. Phys. **133**, 144510 (2010).

[18]B. Baranyi and L. Turi, J. Chem. Phys. **151**, 204304 (2019).

[19]M.-K. Tsai and K. D. Jordan, J. Phys. Chem. A **108**, 2912 (2004).

[20]T. Sommerfeld and K. M. Dreux, J. Chem. Phys. **137**, 244302 (2012).

[21]M. E. Castellani, C. S. Anstöter, and J. R. R. Verlet, Phys. Chem. Chem. Phys. **21**, 24286 (2019).

[22]J. V. Ortiz, V. G. Zakrzewski, and O. Dolgounitcheva, in *Conceptual trends in Quantum Chemistry*, edited by E. Kryachko (Kluwer, Dordrecht, 1997).

[23]T. Sommerfeld, J. Chem. Theory Comput. **9**, 4866 (2013).

[24]A. Bondi, J. Phys. Chem. **68**, 441 (1964).

[25]T. H. Dunning Jr., J. Chem. Phys. **90**, 1007 (1989).

[26]E. Papajak, J. Zheng, X. Xu, H. R. Leverentz, and D. G. Truhlar, J. Chem. Theory Comput. **7**, 3027 (2011).

[27]P. Skurski, M. Gutowski, and J. Simons, Int. J. Quant. Chem. **80**, 1024 (2000).

[28]M. Nooijen and R. J. Bartlett, J. Chem. Phys. **102**, 3629 (1995).

[29]D. A. Matthews and J. F. Stanton, J. Chem. Phys. **145**, 124102 (2016).

[30]F. Neese, Wiley Interdisciplinary Reviews: Computational Molecular Science **2**, 73 (2012).

[31]F. Neese, Wiley Interdisciplinary Reviews: Computational Molecular Science **8**, e1327 (2017).

[32]R. M. Parrish, L. A. Burns, D. G. A. Smith, A. C. Simmonett, A. E. DePrince III, E. G. Hohenstein, U. Bozkaya, A. Y. Sokolov, R. D. Remigio, R. M. Richard, J. F. Gonthier, A. M. James, H. R. McAlexander, A. Kumar, M. Saitow, X. Wang, B. P. Pritchard, P. Verma, H. F. Schaefer III, K. Patkowski, R. A. King, E. F. Valeev, F. A. Evangelista, J. M. Turney, T. D. Crawford, and C. D. Sherrill, J. Chem. Theory Comput. **13**, 3185 (2017).

[33]J. F. Stanton, J. Gauss, L. Cheng, M. E. Harding, D. A. Matthews, and P. G. Szalay, "CFOUR, Coupled-Cluster techniques for Computational Chemistry, a quantum-chemical program package," With contributions from A.A. Auer, R.J. Bartlett, U. Benedikt, C. Berger, D.E. Bernholdt, Y.J. Bomble, O. Christiansen, F. Engel, R. Faber, M. Heckert, O. Heun, M. Hilgenberg, C. Huber, T.-C. Jagau, D. Jonsson, J. Jusélius, T. Kirsch, K. Klein, W.J. Lauderdale, F. Lipparini, T. Metzroth, L.A. Mück, D.P. O'Neill, D.R. Price, E. Prochnow, C. Puzzarini, K. Ruud, F. Schiffmann, W. Schwalbach, C. Simmons, S. Stopkowicz, A. Tajti, J. Vázquez, F. Wang, J.D. Watts and the integral packages MOLECULE (J. Almlöf and P.R. Taylor), PROPS (P.R. Taylor), ABACUS (T. Helgaker, H.J. Aa. Jensen, P. Jørgensen, and J. Olsen), and ECP routines by A. V. Mitin and C. van Wüllen. For the current version, see http://www.cfour.de.

[34]MRCC, A quantum chemical program suite written by M. Kállay, P. R. Nagy, Z. Rolik, D. Mester, G. Samu, J. Csontos, J. Csóka, B. P. Szabó, L. Gyevi-Nagy, I. Ladjánszki, L. Szegedy, B. Ladóczki, K. Petrov, M. Farkas, P. D. Mezei, and B. Hégely. See also Z. Rolik, L. Szegedy, I. Ladjánszki, B. Ladóczki, and M. Kállay, *J. Chem. Phys.* **139**, 094105 (2013), as well as: www.mrcc.hu.

[35]F. Jensen, J. Chem. Phys. **117**, 9234 (2002).

[36]W. R. Garrett, J. Chem. Phys. **69**, 2621 (1978).

[37]H. Abdoul-Carime and C. Desfrançois, Eur. Phys. J. D **2**, 149 (1998).

[38]C. Desfrançois, H. Abdoul-Carime, and J.-P. Schermann, Int. J. Mol. Phys. B **10**, 1339 (1996).

[39]H. Liu, C. Ning, D. Huang, P. D. Dau, and L. Wang, Angew. Chem., Int. Ed. **52**, 8976 (2013).

TABLE I. Systematic names of amine N-oxides studied and compact formulas used in the rest of the paper. Note that syn ethylamine N-oxide does not represent a conformer, but a conformation, and is therefore labeled with its torsion angle 0°.

Name	Conformer	Formula
amine N-oxide		H_3NO
methylamine N-oxide		MeH_2NO
dimethylamine N-oxide		Me_2HNO
ethylamine N-oxide	anti	EtH_2NO-a
	gauche	EtH_2NO-g
	syn	EtH_2NO-0
trimethylamine N-oxide		Me_3NO
ethylmethylamine N-oxide	anti	EtMeHNO-a
	gauche-1	EtMeHNO-g1
	gauche-2	EtMeHNO-g2
isopropylamine N-oxide	anti-gauche	$iPrH_2NO$-ag
	gauche-gauche	$iPrH_2NO$-gg
propylamine N-oxide	anti-anti	$nPrH_2NO$-aa
	anti-gauche	$nPrH_2NO$-ag
	gauche-gauche-1	$nPrH_2NO$-gg1
	gauche-gauche-2	$nPrH_2NO$-gg2
tert-butylamine N-oxide		$tBuH_2NO$
piperidine N-oxide	axial	aPNO
	equatorial	ePNO
phenylamine N-oxide		PhH_2NO
methylphenylamine N-oxide		PhMeHNO
dimethylphenylamine N-oxide		$PhMe_2NO$
diphenylamine N-oxide		Ph_2HNO
methyldiphenylamine N-oxide		Ph_2MeNO
triphenylamine N-oxide		Ph_3NO

TABLE II. Electron binding energies in meV of four N-oxides (see Tab. I) computed with various different *ab initio* methods.

	H_3NO	MeH_2NO	aPNO	PhH_2NO
KT	53.5	22.6	6.66	7.33
HF	59.3	24.6	6.72	8.16
MP2	98.5	36.8	13.0	18.0
OO-MP2	123.9	54.7	29.0	47.6
CCSD	116.1	53.6	25.9	36.6
CCSD(T)	123.1	57.0	28.1	40.0
CCSDT	125.0	58.5	—	—
CCSDT[Q]	124.4	58.1	—	—
CCSDT(Q)	125.6	58.9	—	—
EOM-CCSD(2)	121.1	60.3	29.5	43.1
EOM-CCSD	121.4	58.3	28.0	42.0
EOM-CCSD*	127.9	60.1	29.3	45.6
EOM-CCSD(T)(a)*	125.9	59.0	30.1	43.3
EOM-CCSD(T)(a)	128.1	60.9	—	—
EOM-CCSDT	126.9	59.9	—	—

TABLE III. *Ab initio* results and excluded volume descriptors. Table entries are ordered by molar mass and isomer. The polarizability is the isotropic value, and the excluded volume descriptors $V_x^{(i)}$ are expressed in terms of the respective "reference" volume for H_3NO obtained with the same model.

	E_b	E_b	E_b	μ	α	$V_x^{(1)}$	$V_x^{(2)}$	$V_x^{(3)}$	$\langle r_+ \rangle$	$\langle r_+ \rangle$
	KT	EOM-CCSD	OO-MP2	MP2	MP2	model	model	model	SCF	EOM
	meV	meV	meV	D	Å^3	V_x^{ref}	V_x^{ref}	V_x^{ref}	Å	Å
H_3NO	52.6	121.4	123.9	5.502	2.85	1.00	1.00	1.00	9.5	6.4
MeH_2NO	23.0	58.2	54.7	5.370	4.67	1.92	2.42	1.59	14.6	9.1
Me_2HNO	13.9	36.6	33.3	5.209	6.41	2.76	3.71	2.12	18.3	11.2
EtH_2NO-a	16.7	46.9	45.4	5.708	6.38	4.06	5.82	2.15	17.8	10.6
EtH_2NO-g	15.6	47.3	44.3	5.123	6.37	2.17	2.81	1.69	17.2	9.8
EtH_2NO-0	15.4	48.9	45.4	5.031	6.30	2.30	3.02	1.70	17.0	9.6
Me_3NO	9.3	29.1	28.1	5.058	8.08	3.51	4.88	2.59	21.1	12.2
EtMeH-a	11.4	32.1	29.9	5.436	8.10	4.75	6.89	2.58	17.8	10.6
EtMeH-g1	9.2	28.2	24.8	4.918	8.14	3.09	4.23	2.21	17.2	9.8
EtMeH-g2	9.9	31.3	28.8	4.964	8.05	3.11	4.27	2.22	17.0	9.6
$iPrH_2NO$-ag	11.5	37.1	35.5	5.374	8.09	4.46	6.46	2.28	20.3	11.5
$iPrH_2NO$-gg	11.6	46.6	45.4	4.918	8.06	2.69	3.64	1.81	19.2	9.8
$nPrH_2NO$-aa	13.6	40.7	39.3	5.860	8.16	5.68	8.03	2.18	19.8	11.5
$nPrH_2NO$-ag	14.2	42.1	42.1	5.935	8.09	6.10	8.95	2.44	19.7	11.5
$nPrH_2NO$-gg1	13.9	48.3	45.8	4.977	8.09	2.38	3.14	1.72	17.9	9.7
$nPrH_2NO$-gg2	11.4	40.4	38.3	4.971	8.05	2.76	3.74	1.79	19.5	10.5
$tBuH_2NO$	8.6	34.6	34.2	5.092	9.78	4.87	7.11	2.41	22.1	11.6
aPNO	5.3	29.4	29.0	4.842	10.68	3.88	5.48	2.33	25.3	12.3
ePNO	11.5	36.2	36.8	5.855	10.79	7.56	11.28	2.98	21.4	12.4
PhH_2NO	7.3	42.0	47.6	4.994	12.41	5.68	7.87	2.08	24.5	10.7
PhMeHNO	6.7	29.0	32.6	4.754	14.20	6.32	8.87	2.57	27.9	12.8
$PhMe_2NO$	3.7	23.9	27.1	4.526	15.89	6.86	9.74	2.96	32.9	13.7
Ph_2HNO	2.6	22.1	30.3	4.732	22.26	9.28	13.15	2.87	39.8	—
Ph_2MeNO	1.5	18.3	25.6	4.284	23.91	9.56	13.64	3.21	47.1	—
Ph_3NO	0.7	—	20.9	3.971	32.15	12.07	17.27	3.39	69.1	—

TABLE IV. Results from fitting QSPRs defined in eqs.(8), (9) and (10) to the KT electron binding energies listed in Tab. III. The first entry in every table cell is the mean absolute errror (see eq.(12)). The parameters are in units so that the dipole unit is D, the excluded volumes are measured on a scale relative to H_3NO, and E_b is in meV.

	V_x^1	V_x^2	V_x^3
eq. (8)	7.9%	7.5%	13.8%
	$A = 7.30 \cdot 10^4$	$A = 1.00 \cdot 10^5$	$A = 7.28 \cdot 10^4$
	$B = 14.8$	$B = 15.2$	$B = 14.3$
	$m = 0.830$	$m = 0.753$	$m = 1.86$
eq. (9)	7.8%	7.5%	12.7%
	$A = 6.33 \cdot 10^2$	$A = 3.08 \cdot 10^4$	$A = 3.45 \cdot 10^9$
	$B = 10.4$	$B = 14.1$	$B = 24.3$
	$C = 1.28$	$C = 0.324$	$C = -2.88$
	$m = 0.855$	$m = 0.765$	$m = 1.78$
eq. (10)	7.9%	7.7%	14.7%
	$A = 0.180$	$A = 0.181$	$A = 0.274$
	$n = 4.01$	$n = 4.10$	$n = 3.88$
	$m = 0.863$	$m = 0.780$	$m = 1.91$

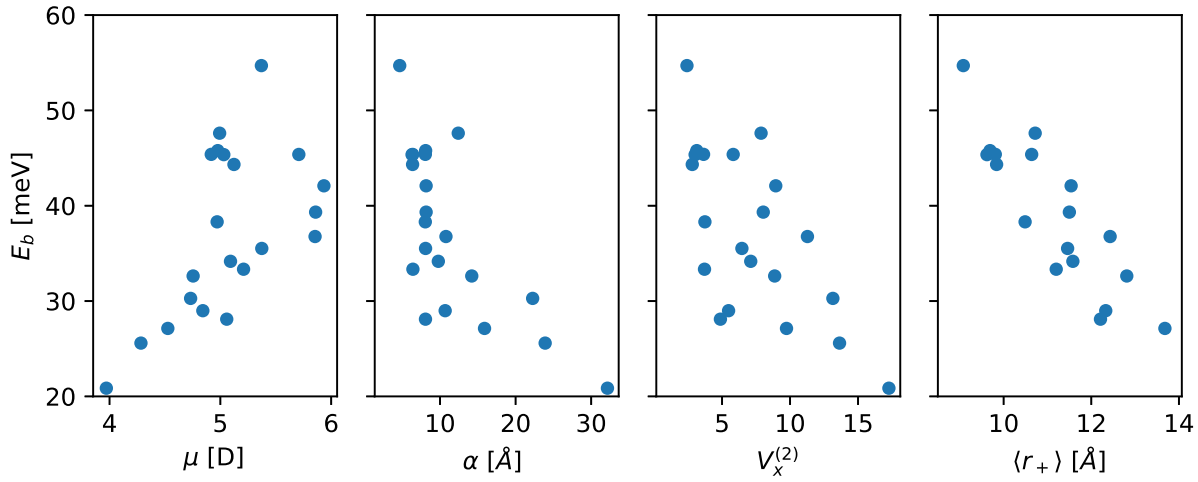

FIG. 1. Dependency of the binding energy E_b on the dipole moment μ, the isotropic polarizability, and selected excluded volume descriptors defined in eqs.(2) and (1). The binding energy of H_3NO is omitted since it represents a dramatic outlier showing an E_b more than twice as large as the next smaller value. The displayed valued were obtained using ΔOO-MP2 (E_b), MP2 (μ and α), and the EOM-CCSD natural orbitals ($\langle r_+ \rangle$).

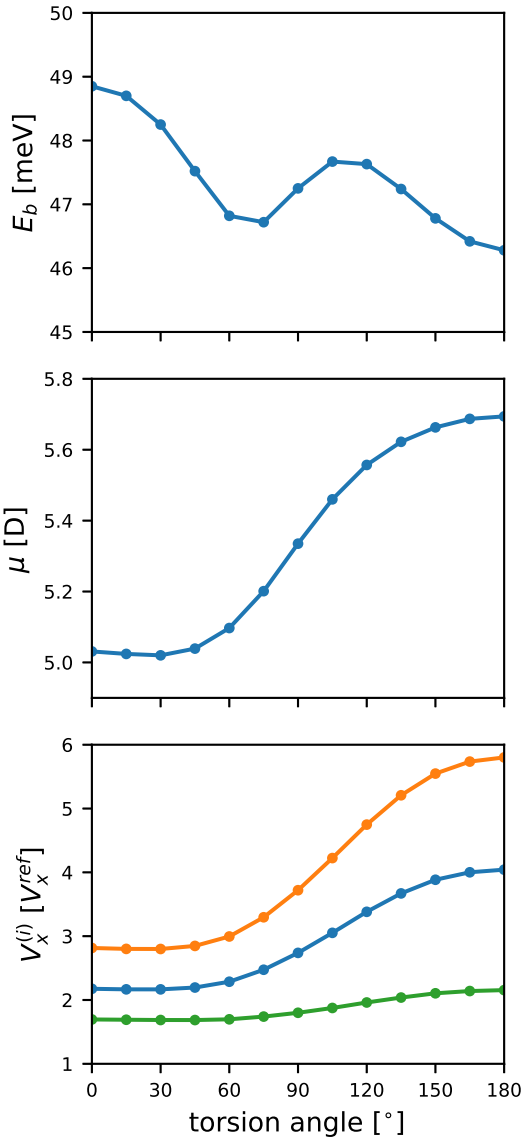

FIG. 2. Binding energy, dipole, and excluded volume descriptors of EtH_2NO in dependence of the O–N–C–C torsion angle θ. The associated computational methods are: EOM-CCSD for E_b, MP2 for μ, and our models $V_x^{(i)}$ (see eq.(2)) (1, 2, 3 shown in blue, orange, and green). As in Tab. III, $V_x^{(i)}$ is expressed relative to the respective values for H_3NO.

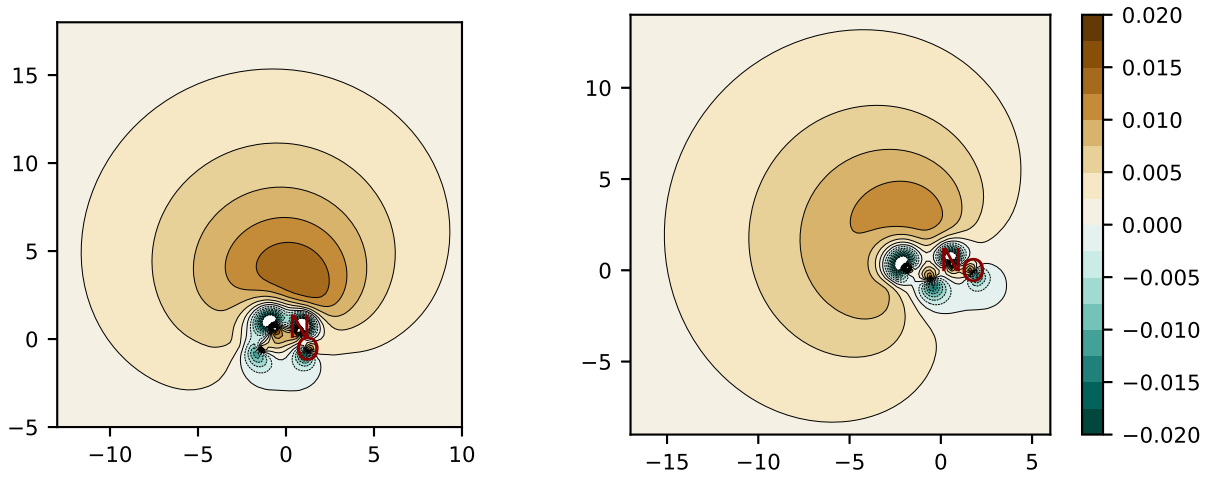

FIG. 3. Cuts through EOM-CCSD natural orbitals describing the excess electron for the syn ($\theta = 0°$; left panel) and anti ($\theta = 180°$; right panel) conformations of EtH_2NO. All non-hydrogen atoms lie in the cutting plane. The units on the length axes are Å and both panels show a 25 by 25Å area. The outermost contour line drawn corresponds to 0.0025 $Bohr^{-3/2}$ and the densities enclosed by this iso-contour are 76% and 70%, respectively.

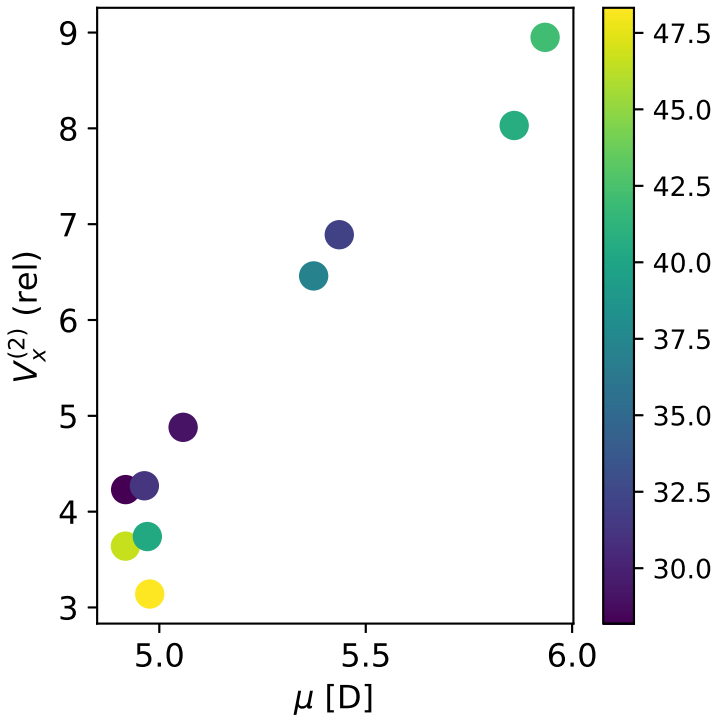

FIG. 4. Binding energy (color coded, meV) of ten $C_3H_{10}NO$ isomers and conformers in dependence of their dipole moment and their excluded volume.

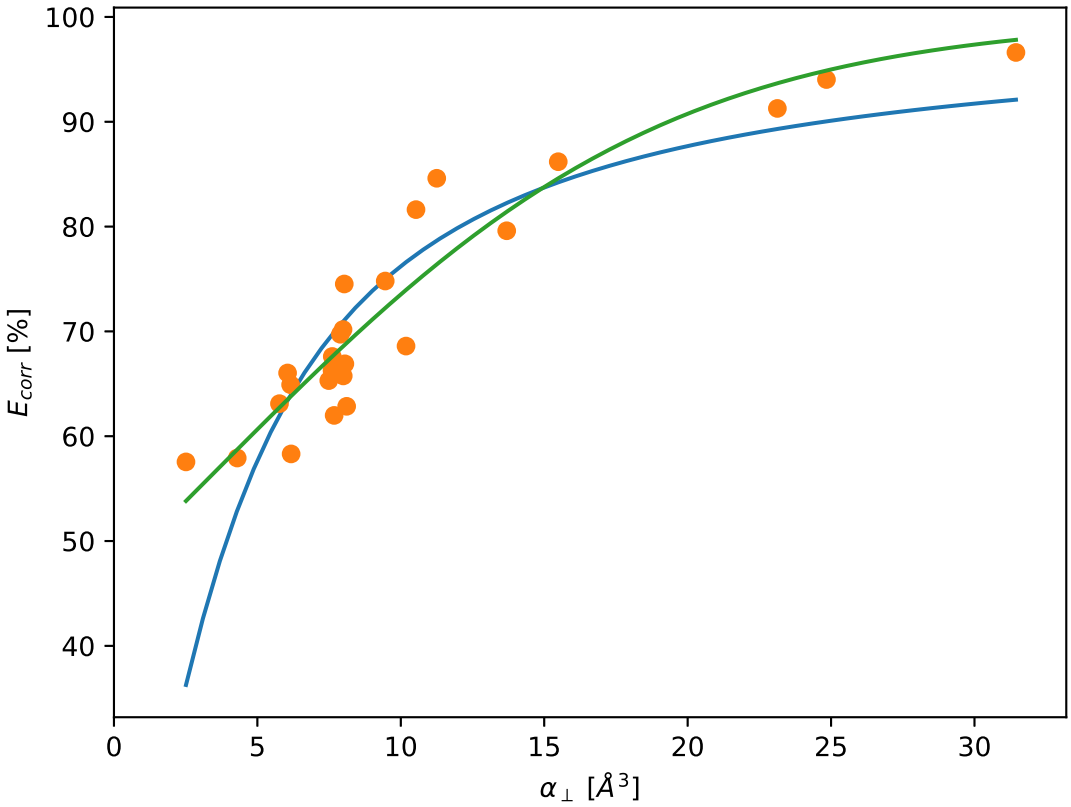

FIG. 5. Correlation contribution to the binding energy *vs.* the average polarizability orthogonal to the molecular dipole, $\alpha_\perp$. The orange circles represent the *ab initio* results (c.f. Tab. III), and the green and blue lines represent the one and three parameter fits with an arctan and a logistic function, respectively (see eqs.(15) and (16)).